One-dimensional walls in liquid crystals

M. Simões*
Departamento de Fisica, Universidade Estadual de Londrina, Campus Universitario, 86051-970 Londrina, PR, Brazil
(Received 7 April 1997)

We study the geometry of the matter flow which leads to the formation of one-dimensional walls above the magnetic Fréedericksz threshold in some nematic materials. The corresponding anisotropic Navier-Stokes equation, subject to the appropriate boundary conditions, is solved. We show analytically that the one-dimensional nature of the observed walls arises from the combination of the planar geometry of the director, imposed before the magnetic field is turned on, the anisotropic viscosity of the nematic material, and the saturated profile of the director along the direction of the magnetic field. The matter flow along the direction perpendicular to the magnetic field is analytically studied, and the conditions that restrict it to the edge of the sample are shown. The influence of this transverse flow of matter on the bending profile of the director is also analyzed. [S1063-651X(97)10509-8]

PACS number(s): 61.30.Gd, 61.30.Jf, 64.70.Md

I. INTRODUCTION

Walls are the structures usually found in nematic liquid crystals (NLC's), formed under the action of an external field [1] that makes the transition between adjacent symmetrical distorted textures. They have been widely investigated from both theoretical and experimental points of view [2–9]. Their practical importance, besides being typical examples of textures in NLC's, lies on the fact that under simple experimental conditions the measurements of their parameters can show the elastic constant values as well as the magnetic susceptibility of the NLC [10,11].

When a magnetic field is used as the external inductor, these walls arise from the combined action of the external field and the matter movement that happens as soon as the magnetic field is turned on above the Fréedericksz threshold. In a remarkable work, Lonberg *et al.* [5] showed how this interesting mechanism works: the external magnetic field rotates the director stimulating the fluid flow, which in turn generates a nonuniform rotation pattern in the director reinforcing the opposite rotations of the neighboring regions of the sample. They were able to show that by this mechanism the wall formation has an effective lower viscosity than the matter movement forming the homogeneous alignment [5]. One important characteristic of these structures is that they appear as a periodic one-dimensional pattern perpendicular to the external magnetic field. It was shown that this periodicity follows directly from its dimension [12].

Even though the formation of these structures is well understood both theoretically and experimentally [5,13,14], a careful analysis of the matter flow geometry taking into account the effect of the boundary conditions is still needed. So far this phenomenon has been studied, taking into account the bulk properties, and has not considered the physics at the edges of the sample. For example, it is known that the matter movement in the direction perpendicular to the magnetic field must be restricted to the neighborhoods of the sample edges [5], but a clear analysis of the causes and influences of this perpendicular matter movement on the director profile is still to be carried out. Furthermore, it has been observed that walls formed under these conditions are one dimensional. But what are the characteristics of the system that make these striking patterns possible? Lonberg *et al.* stressed the role of the anisotropy in the viscosity coefficients. In the present study we stress the importance of the director profile along the direction of the magnetic field. We will solve the anisotropic linear Navier-Stokes equation with the appropriated boundary conditions, supposing that the matter movement is restricted to the plane of the sample. With this solution we will be able to study the director bending profile throughout the sample.

II. FUNDAMENTALS

Considering that NLC's can be described by a continuum model whose elastic energy is given by the Frank free energy [1], and whose motion is described by the so-called Ericksen, Leslie, and Parodi (ELP) approach [1,15,16], we will choose a particular geometry for our analyses which includes a slab with dimensions a along the x axis, b along the y axis, and d along the z axis, in such a way that $a \gg b \gg d$. In our analysis, the director is previously prepared in such a way that it is initially uniformly aligned along the $\vec{e_x}$ direction. An external controlled magnetic field H is applied along the y axis. In order to describe the texture produced in the nematic material, we will assume that the components of the director could be expressed by the planar geometry

$$n_x = \cos\theta(x,y,z), \quad n_y = \sin\theta(x,y,z), \quad n_z = 0, \qquad (1)$$

where $\theta(x,y,z)$ is the angle between the director $\vec{n}$ and the $\vec{e_x}$ direction.

The expression of the total free energy in the two elastic constant approximation ($K_{11} = K_{33}$), taking into account the magnetic-field coupling, is [1,3]

$$F = \int_V \{ \tfrac{1}{2} K_{33} [(\partial_x \theta)^2 + (\partial_y \theta)^2] + \tfrac{1}{2} K_{22} (\partial_z \theta)^2 - \tfrac{1}{2} \chi_a H^2 \sin^2\theta \} dV, \qquad (2)$$

*Electronic address: simoes@npd.uel.br

where K_{11}, K_{22}, and K_{33} are the elastic constants of splay, twist, and bend, respectively, and V is the volume of the sample.

The motion of the nematic fluid will be described using the anisotropic version of the Navier-Stokes equation

$$\rho\left(\frac{\partial \mathcal{V}_\alpha}{\partial t}+\mathcal{V}_\beta\frac{\partial \mathcal{V}_\alpha}{\partial x_\beta}\right)+\frac{\partial}{\partial x_\beta}(-p\,\delta_{\alpha\beta}+\sigma_{\beta\alpha}), \tag{3}$$

where ρ is the density of the system, $\mathcal{V}_\alpha$ the α component of the velocity, p is the pressure, and $\sigma_{\beta\alpha}$ is the associated anisotropic stress tensor [16].

Finally, the equation for the motion of the director will be represented as [15]

$$I\frac{d\vec{\Omega}}{dt}=\vec{\Gamma}_F+\vec{\Gamma}_{\rm visc}, \tag{4}$$

where I is the moment of inertia per unit volume; $\vec{\Omega}$ is the local angular velocity of the director; $\vec{\Gamma}_F$ is the torque per unite volume on the director due to the elastic forces, i.e.,

$$\vec{\Gamma}_F=\vec{n}\times\vec{h}, \tag{5}$$

where $\vec{h}$ is the molecular field [1]; and $\vec{\Gamma}_{\rm visc}$ is given by [15]

$$\vec{\Gamma}_{\rm visc}=-\gamma_1\vec{n}\times\vec{N}-\gamma_2\vec{n}\times\overrightarrow{A\cdot n}, \tag{6}$$

where $N_\alpha=d_t n_\alpha-(\vec{\omega}\times\vec{n})_\alpha$, $\vec{\omega}=\frac{1}{2}\vec{\nabla}\times\vec{\mathcal{V}}$, γ_1 and γ_2 are the shear torque coefficients and $\overrightarrow{A\cdot n}$ is a notation for the scalar product of the tensor $A_{\alpha\beta}=\frac{1}{2}(\partial_\alpha\mathcal{V}_\beta+\partial_\beta\mathcal{V}_\alpha)$ with the vector $\vec{n}$ [1,15,16]. We will also consider, as usual, the fluid incompressible

$$\partial_\alpha\mathcal{V}_\alpha=0. \tag{7}$$

The condition $a\gg b\gg d$ will allow us to restrict our dynamical analysis to the (x,y) plane, and work with an approximation that, even after the turning on of the magnetic field, there will be no matter motion along the $\vec{e_z}$ direction, that is $\mathcal{V}_z=0$ and $n_z=0$. Thus, the known phenomenology happening along the $\vec{e_z}$ direction will not be considered here [13,14]. Furthermore we will consider that the velocity of the matter in the sample is such that we can neglect the nonlinear term in the Navier-Stokes equation. In this way, using Eq. (7) and computing the stress tensor in the small bending approximation, the two components of Eq. (3) become

$$\rho\partial_t\mathcal{V}_x=-\partial_x p+(A_1-A_2)\partial_x^2\mathcal{V}_x+A_3\partial_y^2\mathcal{V}_x+A_3\partial_z^2\mathcal{V}_x+A_4\partial_y\dot{\theta}, \tag{8}$$

$$\rho\partial_t\mathcal{V}_y=-\partial_y p+(A_5-A_2)\partial_y^2\mathcal{V}_y+A_6\partial_x^2\mathcal{V}_y+\frac{A_5}{2}\partial_z^2\mathcal{V}_y+A_7\partial_x\dot{\theta},$$

where $A_1=\alpha_1+\alpha_4+\alpha_5+\alpha_6$, $A_2=\frac{1}{2}(\alpha_2+\alpha_4+\alpha_5)$, $A_3=\frac{1}{2}(\alpha_3+\alpha_4+\alpha_6)$, $A_4=\alpha_3$, $A_5=\alpha_4$, $A_6=\frac{1}{2}(\alpha_1-\alpha_2+\alpha_5)$, $A_7=\alpha_2$, and α_i are the Leslie coefficients [1].

In the planar geometry so far defined, Eq. (4) becomes

$$\begin{aligned}Id_t^2\theta+\gamma_1 d_t\theta=&\gamma_1 W_{xy}-\gamma_2[A_{xy}(n_x^2-n_y^2)+(A_{xx}-A_{yy})n_x n_y]\\&+K_{33}[(\partial_x^2\theta)+(\partial_y^2\theta)]+K_{22}(\partial_z^2\theta)\\&+\chi_a H^2 n_x n_y,\end{aligned} \tag{9}$$

where A_{xy} was defined above and $W_{xy}=\frac{1}{2}(\partial_x\mathcal{V}_y-\partial_y\mathcal{V}_x)$.

III. BEGINNING OF THE PROCESS

Suppose that the magnetic field is turned on just above, but not far from, the Fréedericksz threshold. There will be a time interval close enough to the initial instant in such a way that the bending of the director and the matter movement will be very small. Thus we can consider

$$\theta=\alpha(t)\cos kx\,\sin\left(\frac{\pi}{b}y\right)\sin\left(\frac{\pi}{d}z\right),\quad d_t^2\theta\simeq 0,$$

$$W_{ij}\simeq A_{ij}\simeq 0. \tag{10}$$

In this approximation, Eq. (9) gives

$$\gamma_1 d_t\alpha=F\alpha, \tag{11}$$

where $F=(\chi_a H^2-K_{33}[k^2+(\pi/b)^2]-K_{22}(\pi/d)^2)$.

Therefore we have

$$\alpha=\alpha_0 e^{(F/\gamma_1)t}, \tag{12}$$

which shows us that the fluctuations will grow exponentially to $F>0$, and will be exponentially damped otherwise. The maximum of this exponential growth, $k\to 0$, reflects the celebrated homogeneous Fréedericksz transition [17]. It should be noted that this exponential growth is governed by the coefficient γ_1. As will be shown further, the nonhomogeneous director bending only happens due to a reduction in the viscosity coefficient via the existence of a $k\neq 0$ which maximizes the exponential growth [5].

With this result we can study the geometry of the nematic fluid matter in these initial instants. With these approximations, Eq. (8) becomes

$$\begin{aligned}\rho\partial_t\mathcal{V}_x&=A_4\partial_y\dot{\theta},\\ \rho\partial_t\mathcal{V}_y&=A_7\partial_x\dot{\theta}.\end{aligned} \tag{13}$$

By imposing $\mathcal{V}_x=\mathcal{V}_y=0$ at $t=0$, we have

$$\mathcal{V}_x=\frac{\pi}{b}\alpha_0 A_4(e^{(F/\gamma_1)t}-1)\cos kx\,\cos\left(\frac{\pi}{b}y\right)\sin\left(\frac{\pi}{d}z\right), \tag{14}$$

$$\mathcal{V}_y=-k\alpha_0 A_8(e^{(F/\gamma_1)t}-1)\sin kx\,\sin\left(\frac{\pi}{b}y\right)\sin\left(\frac{\pi}{d}z\right). \tag{15}$$

So in the initial moments the velocities increase exponentially, and at the center of the sample (around $y\approx b/2$) we have $\mathcal{V}_x\approx 0$. Therefore the matter movement at these points is restricted to the $\vec{e_y}$ direction. Furthermore, for the *N*-(*p*-methoxybenzylidene)-*p*-butylaniline (MBBA), for example, we have $A_7/A_4\approx 10^2$, which, by Eq. (13), im-

plies that any attempt to put the fluid in movement will have a reaction in the $\vec{e_y}$ direction that overcomes the one in the $\vec{e_x}$ direction by this same value.

IV. MATTER FLOW

In this section we will obtain an exact solution for the linearized anisotropic Navier-Stokes equation given in Eq. (8). We will suppose that the exponential increase of the velocity shown above is such that we can neglect the terms $\partial_t \mathcal{V}_x$ and $\partial_t \mathcal{V}_y$, so that the equations for the matter flow become

$$(A_1-A_2)\partial_x^2\mathcal{V}_x+A_3\partial_y^2\mathcal{V}_x+A_3\partial_z^2\mathcal{V}_x=\partial_x p-A_4\partial_y\dot{\theta}, \quad (16)$$

$$(A_5-A_2)\partial_y^2\mathcal{V}_y+A_6\partial_x^2\mathcal{V}_y+\frac{A_5}{2}\partial_z^2\mathcal{V}_y=\partial_y p-A_7\partial_x\dot{\theta}, \quad (17)$$

$$\partial_x\mathcal{V}_x+\partial_y\mathcal{V}_y=0. \quad (18)$$

As we have three linear equations and three unknown variables (the two components of the velocity and the pressure), this system has a solution. Its boundary conditions must assert that the fluid motion is absent at the boundaries of the sample [18]. In this way we will consider that the solution of this set of differential equations has the following forms:

$$\mathcal{V}_x=V_x\ \cos kx C(y)\sin\left(\frac{\pi}{d}z\right), \quad (19)$$

$$\mathcal{V}_y=V_y\ \sin kx S(y)\sin\left(\frac{\pi}{d}z\right), \quad (20)$$

$$p=p_o\ \sin kx P(y)\sin\left(\frac{\pi}{d}z\right), \quad (21)$$

where $C(y)$, $S(y)$, and $P(y)$ will be found using the equations above and the boundary conditions

$$C(0)=C(b)=0,$$

$$S(0)=S(b)=0. \quad (22)$$

It should be noted that along the $\vec{e_x}$ direction periodic boundary conditions are imposed which, together with the hypothesis $a\gg b\gg d$, allow us to consider a system infinitely longer along this direction, leading to a quasicontinuous spectrum to k.

We begin by using the continuity equation. By inserting Eqs. (19) and (20) into Eq. (18), we obtain

$$V_y\partial_y S(y)-kV_x C(y)=0, \quad (23)$$

and by supposing that $S(y)$ and $C(y)$ satisfy the relation

$$\partial_y S(y)=\frac{\pi}{b}\,C(y), \quad (24)$$

and the equation of the continuity becomes

$$-kV_x+\frac{\pi}{b}\,V_y=0, \quad (25)$$

that links the solutions of Eqs. (16) and (17). Suppose that the director has a small bending and strong anchoring at the surface, in such a way that θ can take the form

$$\theta=\alpha\ \cos kx\ \sin\frac{\pi}{b}y\ \sin\frac{\pi}{d}z. \quad (26)$$

By putting Eqs. (19) and (20) into Eqs. (16) and (17), we obtain

$$\left\{A_3\partial_y^2 C(y)-\left[(A_1-A_2)k^2+A_3\left(\frac{\pi}{d}\right)^2\right]C(y)\right\}V_x$$

$$=kp_o P(y)-\frac{\pi}{b}A_4\dot{\alpha}\ \cos\frac{\pi}{b}y, \quad (27)$$

$$\left\{(A_5-A_2)\partial_y^2 S(y)-\left[A_6k^2+\frac{A_5}{2}\left(\frac{\pi}{d}\right)^2\right]S(y)\right\}V_y$$

$$=p_o\partial_y P(y)+kA_7\dot{\alpha}\ \sin\frac{\pi}{b}y. \quad (28)$$

At this point our system is composed of the Eqs. (24), (25), (27), and (28), subjected to the boundary conditions given in Eq. (22). To solve it we differentiate the result of the substitution of Eq. (24) in Eq. (27) in relation to y, and use Eqs. (25) and (28) to obtain

$$\{a_4\partial_y^4 S(y)-a_2\partial_y^2 S(y)+a_0 S(y)\}V_y=a\dot{\alpha}\ \sin\frac{\pi}{b}y, \quad (29)$$

where $a_4=A_3$, $a_2=[(A_1+A_5-2A_2)k^2+A_3(\pi/d)^2]$, $a_0=k^2[A_6k^2+(A_5/2)(\pi/d)^2]$, and $a=k[A_4(\pi/b)^2-A_7k^2]$.

Thus we have reduced our problem to only one linear differential equation with the boundary conditions

$$S(0)=S(b)=0,$$

$$S'(0)=S'(b)=0, \quad (30)$$

whose solution, satisfying these boundary conditions, is given by

$$S(y)=\sin\frac{\pi}{b}y+C_1\cosh\left\{g_1\frac{\pi}{b}\left(y-\frac{b}{2}\right)\right\}$$

$$+C_2\cosh\left\{g_2\frac{\pi}{b}\left(y-\frac{b}{2}\right)\right\}, \quad (31)$$

where

$$C_1=\frac{1}{\cosh\left\{g_1\frac{\pi}{2}\right\}}\,\frac{1}{g_1\tanh\left\{g_1\frac{\pi}{2}\right\}-g_2\tanh\left\{g_2\frac{\pi}{2}\right\}},$$

$$C_2=\frac{1}{\cosh\left\{g_2\frac{\pi}{2}\right\}}\,\frac{1}{g_2\tanh\left\{g_2\frac{\pi}{2}\right\}-g_1\tanh\left\{g_1\frac{\pi}{2}\right\}}, \quad (32)$$

with

$$g_1=\frac{b}{\pi}\left(\frac{a_2+\sqrt{a_2^2-4a_4a_0}}{2a_4}\right)^{1/2},$$

$$g_2=\frac{b}{\pi}\left(\frac{a_2-\sqrt{a_2^2-4a_4a_0}}{2a_4}\right)^{1/2},$$

and $V_y=G\dot{\alpha}$, where $G=a/[a_4(\pi/b)^4+a_2(\pi/b)^2+a_0]$.

In this solution the sine term is the solution of the inhomogeneous equation given in Eq. (29). The remaining terms arise from the solution of its homogeneous part. C_1 and C_2 are chosen in such a way that the sum of the homogeneous and inhomogeneous parts satisfies the boundary conditions given in Eq. (29).

By having the exact solution of Eq. (29), we can evaluate the fluid flow inside the sample. In the example below we will use the Leslie coefficients of MBBA, and will consider $k^2\simeq\frac{1}{2}(\pi/d)^2$. This choice for k^2 is arbitrary. The right way for choosing k^2 will be reviewed below [5]. With these choices we find $g_1\simeq\frac{1}{2}(b/d)$ and $g_2\simeq 2(b/d)$. In Fig. 1 the corresponding graphics for $S(y)$ and $C(y)$ are shown. In this picture it can be noticed that in the center of the sample the fluid movement prevails along the $\vec{e_y}$ direction, while at the borders the movement along the $\vec{e_x}$ direction increases. The pressure resulting in the sample can be easily evaluated by using Eq. (27).

In spite of the fact that Fig. 1 is impressive, it does not show the one-dimensional character of the walls clearly. As was observed by Lomberg *et al.* [5], the fluid flow along the $\vec{e_x}$ direction must be localized at the edges of the sample, and this is not shown by this figure. Indeed there is only one point where the fluid flow is not present along the $\vec{e_x}$ direction: exactly at the center of the slab. We will show that the origin of this shortcoming lies on the profile of the director bending given in Eq. (26). As we assumed that $b\gg d$, there must be a region along the $\vec{e_y}$ direction in which the director bending is constant [1], and this is not described by a sine function. That is, the term $\sin(\pi y/b)$ that appears in Eq. (26) is a poor approximation of the description of the director bending along the $\vec{e_y}$ direction, and must be replaced by a new function. Therefore

$$\theta=\alpha\,\cos kx\,\Sigma(y)\sin\frac{\pi}{d}z, \tag{33}$$

where

$$\Sigma(y)=\begin{cases}\sin\dfrac{\pi}{2l}\,y, & 0\leqslant y<l\\ 1, & l\leqslant y<b-l\\ \sin\dfrac{\pi}{2l}\,(b-y), & b-l\leqslant y\leqslant b;\end{cases} \tag{34}$$

l is the portion along the $\vec{e_y}$ direction where we have the bending in the director direction up to a constant value. In the interval $l\leqslant y\leqslant b-l$ we have the constant bending along the $\vec{e_y}$ direction.

In this case all the calculations follow the same path of the preceding one, and the equation corresponding to the Eq. (29) becomes

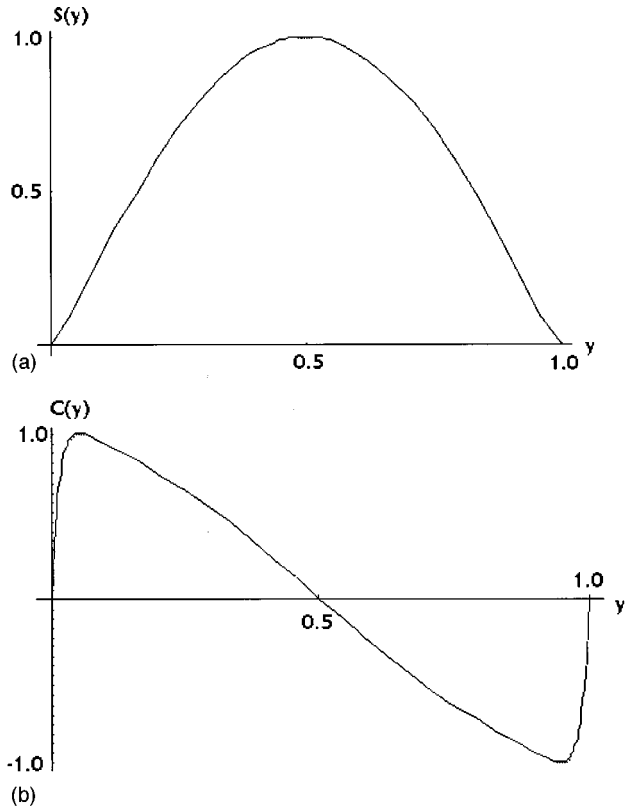

FIG. 1. (a) Profile of the function $S(y)$ along the direction parallel to the external magnetic field. $S(y)$, defined in Eq. (20), is a dimensionless quantity proportional to the velocity along the $\vec{e_y}$ direction. For the $\vec{e_y}$ direction arbitrary length unities were used. Notice that the maximum of the velocity, at the center of the sample, stays in a point. (b) Profile of the function $C(y)$ along the direction parallel to the external magnetic field. $C(y)$, defined in Eq. (19), is a dimensionless quantity proportional to the velocity along the $\vec{e_x}$ direction. For the $\vec{e_y}$ direction arbitrary length unities were used. As we see in Eq. (24), this picture is a derivative of (a); therefore, the velocity along the $\vec{e_x}$ direction increases from the center of the sample to its borders. Meanwhile, due to the boundary conditions, it returns to zero at the sample edges. As it predicts fluid motion of the bulk in the direction perpendicular to the external magnetic field, this profile cannot explain the observed one dimensionality of the walls. As observed by Lomberg *et al.* [5], the velocity along this direction must be localized at the edges of the sample.

$$\{a_4\partial_y^4S(y)-a_2\partial_y^2S(y)+a_0S(y)\}\widetilde{V}_y^i = -b_2\partial_y^2\Sigma(y)-b_0\Sigma(y), \tag{35}$$

where $b_0=\dot{\alpha}k^3A_7$ and $b_2=\dot{\alpha}kA_4$.

The solution of this equation is similar to the one found in Eq. (31), and is given by

$$S(y)=\Sigma(y)+\widetilde{C}_1^i\cosh\left\{g_1\frac{\pi}{b}\left(y-\frac{b}{2}\right)\right\} +\widetilde{C}_2^i\cosh\left\{g_2\frac{\pi}{b}\left(y-\frac{b}{2}\right)\right\}. \tag{36}$$

Now $\widetilde{V}_y^i$, $\widetilde{C}_1^i$, and $\widetilde{C}_2^i$ are not exactly the same given above in Eq. (32). In order to guarantee the continuity of Eqs. (19)

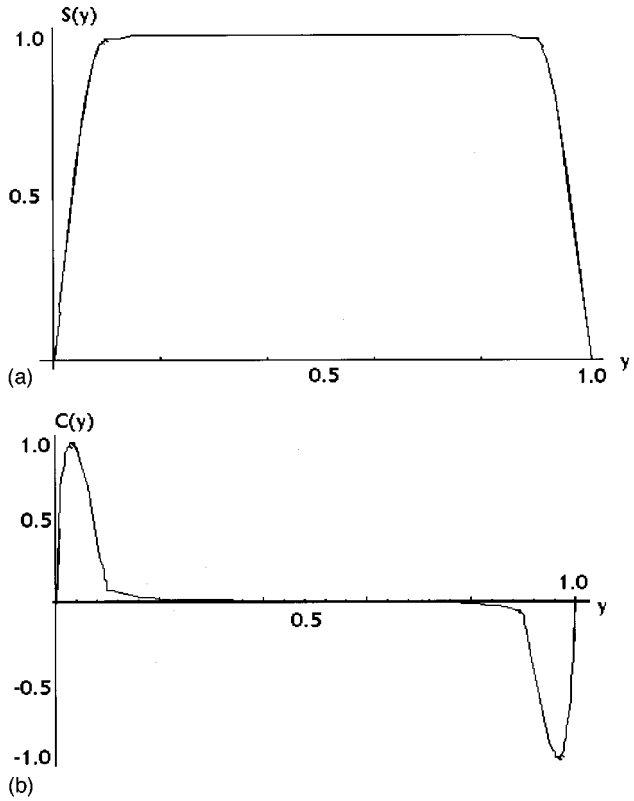

FIG. 2. (a) Profile of the function $S(y)$ along the direction parallel to the external magnetic field when it is assumed, as described in Eqs. (33) and (34), that at the sample center the director has a saturated portion along the $\vec{e_y}$ direction. $S(y)$, defined in Eq. (20), is a dimensionless quantity proportional to the velocity along the $\vec{e_y}$ direction. For the $\vec{e_y}$ direction arbitrary length unities were used. Notice that now the velocity along the $\vec{e_y}$ direction has a saturated portion. In this picture we used $b/d=10$ and $l/b=0.1$. (b) Profile of the function $C(y)$ along the direction parallel to the external magnetic field. $C(y)$, defined in Eq. (19), is a dimensionless quantity proportional to the velocity along the $\vec{e_x}$ direction. For the $\vec{e_y}$ direction arbitrary length unities were used. As we see in Eq. (24), this function is the derivative of the function plotted in Fig. 2(a). Notice that the fluid motion along the $\vec{e_x}$ direction is displaced to the edges to afford an understanding of the one-dimensional pattern of the walls.

and (20), these constants depend on the intervals considered. We use $i=1$ to the symmetric intervals $0\leqslant y\leqslant l$ and $b-l\leqslant y\leqslant b$, and $i=2$ to the interval $l\leqslant y\leqslant b-l$. Indeed in the intervals for which $i=1$ it is enough to make the change $b\rightarrow 2l$ in Eq. (32) in order to obtain the new constants. In the interval for which $i=2$ we have $\tilde{V}_y^2=-b_0/a_0$, $\tilde{C}_1^2=\tilde{C}_1^1+(1/2\tilde{V}_y^1)(\Delta V_y/\Delta G_1)$ and $\tilde{C}_2^2\tilde{C}_2^1-(1/2\tilde{V}_y^1)\ (\Delta V_y/\Delta G_2)$, where $\Delta V_y=\tilde{V}_y^1-\tilde{V}_y^2$, $\Delta G_1=(1/\mathrm{sh}_1)[(g_1/g_2)(\mathrm{ch}_2/\mathrm{sh}_2)-(\mathrm{ch}_1/\mathrm{sh}_1)]$, $\Delta G_2=(1/\mathrm{sh}_2)\times[(g_2\ /g_1)(\mathrm{ch}_1/\mathrm{sh}_1)]-(\mathrm{ch}_2/\mathrm{sh}_2))$, and $\mathrm{sh}_i=\sinh[g_i\pi/b\times(l-b/2)]$, $\mathrm{ch}_i=\cosh[g_i\pi/b(l-b/2)]$.

In Fig. 2 we plot one solution for $S(y)$ and $C(y)$ for $l=0.1$. Notice that, in this figure, we have normalized the interval b to 1. The l represents the fraction of the interval $(0,b)$ in which there is a bending of the director along the $\vec{e_y}$ direction. From Eq. (24) it is easy to see that, as l decreases, or as the constant portion of the director along the $\vec{e_y}$ direction increases, the velocity profile of the fluid along the $\vec{e_x}$ direction becomes more and more concentrated on the edges of the sample. Actually it is not difficult to see from figures 1 and 2 that there is fluid motion along the $\vec{e_x}$ direction only in the portions of the sample where there is the bending portion of $\Sigma(y)$. So as the flat portion of $\Sigma(y)$ increases the fluid flow along the $\vec{e_x}$ direction becomes more and more concentrated on the edges of the sample.

V. DIRECTOR BENDING

Here we discuss how the picture presented previously acts on the bending of the director along the sample. Equation (9) and the fact that the inertial terms can be neglected will be our assumptions. Furthermore we will retain the linear θ terms only. So

$$\gamma_1 d_t\theta=\gamma_1 W_{xy}-\gamma_2 A_{xy}-\gamma_2(A_{xx}-A_{yy})\,\theta + K_{33}[(\partial_x^2\theta)+(\partial_y^2\theta)]+K_{22}(\partial_z^2\theta)+\chi_a H^2\theta. \tag{37}$$

Our first step is the computation of the terms W_{xy}, A_{xy} and $A_{xx}-A_{yy}$, for which we find

$$W_{xy}=(1/2k)V_y\cos kx(k^2S-\partial_y^2 S)\sin(\pi/d\,z);$$

$$A_{xy}=(1/2k)V_y\cos kx(k^2S+\partial_y^2 S)\sin[(\pi/d)\,z]$$

and

$$A_{xx}-A_{yy}=2V_y(\pi/b)\sin kx\,C(y)\sin[(\pi/d)\,z].$$

Furthermore, we notice that

$$\gamma_1 W_{xy}-\gamma_2 A_{xy}=\tfrac{1}{2}(\gamma_1-\gamma_2)kV_y\cos kx\,S(y)\sin\left(\frac{\pi}{d}z\right) - \frac{1}{2k}(\gamma_1+\gamma_2)kV_y\cos kx\,\partial_y^2 S\,\sin\left(\frac{\pi}{d}z\right). \tag{38}$$

But $\gamma_1-\gamma_2=-2\alpha_2$; $\gamma_1+\gamma_2=2\alpha_3$, and $|\alpha_2|\gg|\alpha_3|$ (for the MBBA $|\alpha_2|\sim 10^2|\alpha_3|$) as well as $\partial_y^2 S$ is relevant only in the neighborhoods of the sample edges, where we have $\partial_y^2 S\simeq S(y)$. So we have

$$\gamma_1 W_{xy}-\gamma_2 A_{xy}\simeq\tfrac{1}{2}(\gamma_1-\gamma_2)kV_y\cos kx\,S(y)\sin\left(\frac{\pi}{d}z\right), \tag{39}$$

and use Fig. 2 and Eq. (36) to see that $S(y)$ is well described by $\Sigma(y)$ because it fits very well the velocity of the fluid along the $\vec{e_y}$ direction, as well as its boundary condition that at the edges. The function of the inhomogeneous term in Eq. (36) is just to furnish the appropriated boundary conditions to its derivative [see Eq. (24)], which does not appear in Eq. (39). Thus

$$\gamma_1 W_{xy} - \gamma_2 A_{xy} \simeq \tfrac{1}{2}(\gamma_1 - \gamma_2) k V_y \cos kx \Sigma(y) \sin\left(\frac{\pi}{d} z\right)$$

$$= \tfrac{1}{2}(\gamma_1 - \gamma_2) k V_y \frac{\theta}{\alpha}. \quad (40)$$

By defining $F\theta = K_{33}[(\partial_x^2\theta) + (\partial_y^2\theta)] + K_{22}(\partial_z^2\theta) + \chi_a H^2 \theta$, we obtain, for F,

$$F = \chi_a H^2 - \left\{ K_{33}\left[\left(\frac{\pi}{2l}\right)^2 \delta_{i,1} + k^2\right] - K_{22}\left(\frac{\pi}{d}\right)^2 \right\}, \quad (41)$$

where $\delta_{i,1} = 1$ if the interval under consideration is the interval $i = 1$ defined in Eq. (31), and 0 otherwise.

We then obtain

$$\gamma_1 \dot{\alpha} = \tfrac{1}{2}(\gamma_1 - \gamma_2) k G \dot{\alpha} - 2\gamma_2 \left(\frac{\pi}{b}\right) \sin kx C(y) \sin\left(\frac{\pi}{d} z\right) G \alpha \dot{\alpha}$$

$$+ F\alpha, \quad (42)$$

where we used Eq. (32). So this equation can be rewritten as

$$\dot{\alpha} + \mathcal{M}\alpha\dot{\alpha} - \mathcal{F}\alpha = 0 \quad (43)$$

where

$$\mathcal{M} = \frac{2\gamma_2 \left(\frac{\pi}{b}\right) \sin kx C(y) \sin\left(\frac{\pi}{d} z\right) G}{\gamma_1 - \frac{1}{2}(\gamma_1 - \gamma_2) k G}, \quad (44)$$

$$\mathcal{F} = \frac{F}{\gamma_1 - \frac{1}{2}(\gamma_1 - \gamma_2) k G}. \quad (45)$$

The solution of this equation is given by the transcendental expression

$$\alpha(t) e^{\mathcal{M}\alpha(t)} = \varepsilon e^{\mathcal{F}t}, \quad (46)$$

where ε is a constant of integration.

This is a generalization of the result found by Lomberg *et al.* [5], taking into account the effect of the boundary conditions on the time development of the amplitude $\alpha(t)$. That is, as $\mathcal{M}$ depends on (x,y,z) the growth of $\alpha(t)$ is not constant throughout the sample. By looking at Fig. 2, and considering that $C(y)$ can not be zero only in the neighborhoods of the edges of the sample, we conclude that in the bulk the growth of the amplitude α is given by $\alpha(t) = \varepsilon e^{\mathcal{F}t}$. Notice that the maximum growth rate in this exponential is not given by $k = 0$. As we pointed out in Eq. (12), and clearly showed in Eq. (45), there is a reduction in γ_1 which grows with k. The value of k that affords the maximum growing rate in Eq. (43) is the one chosen by the system. If, in this equation, we make $2l \to b$ and use the fact that $b \gg d$ we will see that $\mathcal{F}$ assumes the form found by Lomberg *et al.* [5].

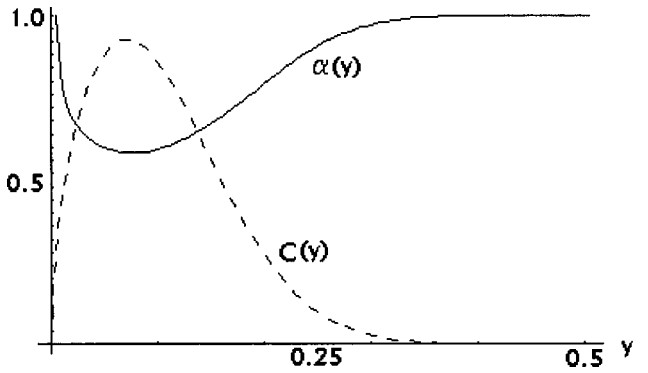

FIG. 3. Superposition of the curves $C(y)$ and as a function of the direction parallel to the external magnetic field. The dashed curve represents the dimensionless quantity $C(y)$, and the continuous curve represents $\alpha(t)$ in arbitrary unities. Notice a reduction in the amplitude growth speed, given by $\alpha(t)$, just at the regions where the velocity of the fluid along the $\vec{e_x}$ direction is present.

So, with Eq. (43), we can study the influence of the sample edges in the development of $\alpha(t)$. Notice that exactly at the edges we have $\mathcal{M} = 0$ and, as we go along the $\vec{e_y}$ direction, $\mathcal{M}$ grows and returns to zero when it reaches distance l from the border of the sample. As we see in Fig. 2, this localized peak is due to the matter flux along the $\vec{e_x}$ direction that, as seen in Eq. (19), presents this same behavior. In Fig. 3 this is illustrated with a superposition of the profiles of $\alpha(t)$ and $C(y)$ near the edges of the sample for the instant at which $\varepsilon e^{\mathcal{F}t} = 1$.

VI. CONCLUSION

In this work we studied the geometry of the matter flow of a NLC sample as an external magnetic field is turned on above the Fréedericksz threshold perpendicular to the initial direction of the planar director. After the linear anisotropic Navier-Stokes equation of the problem was analytically solved, the role of the boundary conditions in the matter flow was studied. It was shown that, like the anisotropy of the viscosity coefficients, the geometry of the sample has a fundamental importance in the understanding of the walls one-dimensional patterns. This happens because a saturated portion of the director along the direction of the external magnetic field is required. It is also shown that the matter movement, in the direction perpendicular to the magnetic field, is restricted to the neighborhoods of the edges of the sample where the bending of the director is not constant.

With these results, the equation of the director bending was solved in the entire sample. We show that the magnitude of the sample dimensions ratios guarantees that, in the central portion of the sample, the result of Lomberg *et al.* [5] is recovered. Meanwhile in the neighborhoods of the sample edges, the time amplitude growth is reduced due to the matter flow in the direction perpendicular to the external magnetic field.

[1] P. G. de Gennes, *The Physics of Liquid Crystals*, 2nd ed. (Clarendon, Oxford, 1993).
[2] W. Helfrich, Phys. Rev. Lett. **21**, 1518 (1968).
[3] F. Brochard, J. Phys. (Paris) **33**, 607 (1972).
[4] L. Léger, Mol. Cryst. Liq. Cryst. **24**, 33 (1973).
[5] F. Lonberg, S. Fraden, A. J. Hurd, and R. B. Meyer, Phys. Rev. Lett. **52**, 1903 (1984).
[6] F. Lonberg and R. B. Meyer, Phys. Rev. Lett. **55**, 718 (1985).
[7] C. Srajer, S. Fraden, and R. B. Meyer, Phys. Rev. A **39**, 9 (1989).
[8] J. Charvolin and Y. Hendrix, J. Phys. (France) Lett. **41**, 597 (1980).
[9] T. Kroin and A. M. Figueiredo Neto, Phys. Rev. A **36**, 2987 (1987).
[10] T. Kroin, A. J. Palangana, and A. M. Figueiredo Neto, Phys. Rev. A **39**, 5373 (1989).
[11] M. Simões, A. J. Palangana, and L. R. Evangelista, Phys. Rev. E **54**, 3765 (1996).
[12] M. Simões, Phys. Rev. E **54**, 6952 (1996).
[13] M. Grigutsch, N. Klöpper, H. Schmiedel, and R. Stannarius, Mol. Cryst. Liq. Cryst. **261**, 283 (1995).
[14] M. Grigutsch, N. Klöpper, H. Schmiedel, and R. Stannarius, Phys. Rev. E **49**, 5452 (1994).
[15] W. H. de Jeu, *Physical Properties of Liquid Crystalline Materials* (Gordon and Breach, New York, 1979).
[16] G. Vertogen and W. H. de Jeu, *Thermotropic Liquid Crystals, Fundamentals* (Springer-Verlag, Berlin, 1988).
[17] L. D. Landau and E. M. Lifshitz, *Fluid Mechanics* (Butterworth-Heinemann, Oxford, 1995).
[18] V. Frederisckz and V. Zolina, Trans. Faraday Soc. **29**, 919 (1933).